Conf-920438--1

STRUCTURE AND FLUX PINNING PROPERTIES OF IRRADIATION DEFECTS IN $YBa_2Cu_3O_{7-x}$*

M. A. Kirk
Materials Science Division
Argonne National Laboratory
Argonne, IL 60439

ANL/CP--76500

DE92 016739

June 1992

INVITED paper to Critical Currents in High T_c Superconductors, April 22-24, 1992, Vienna, Austria: To be published in Journal of Cryogenics.

*This work was supported by the U. S. Department of Energy, Conservation and Renewable Energy, and BES-Materials Sciences, under Contract W-31-109-Eng-38, the National Science Foundation-Office of Science and Technology Center for Superconductivity, under Contract No. STC-8809854, and the Science and Engineering Research Council (U.K.) under grant GR/G43065.

Structure and Flux Pinning Properties of Irradiation Defects In $YBa_2Cu_3O_{7-x}$

M. A. Kirk

Materials Science Division, Argonne National Laboratory, Argonne, IL 60439 USA

KEYWORDS

Superconductivity, YBCO, Irradiation Defects, Flux Pinning, Critical Currents.

ABSTRACT

We review our investigations of defects produced in $YBa_2Cu_3O_{7-x}$ by various forms of irradiation. The defect microstructure has been studied by transmission electron microscopy (TEM). Irradiation enhancements of flux pinning have been studied by SQUID magnetometry on single crystals. In many cases the same single crystals were used in both TEM and SQUID investigations. The primary atom recoil spectra for all the irradiations studied (fission neutrons, MeV protons, MeV electrons, and GeV ions) have been carefully calculated and used to correlate the TEM and magnetization results for the different types of irradiation. Correlation of annealing experiments, employing both TEM and SQUID measurements, among several types of irradiation has also yielded information on the different defect structures present. Defect densities, sizes and strain field anisotropies have been determined by TEM. Defect flux pinning anisotropies have been determined for two field orientations (H II c and H II ab) in twinned single crystals. The temperature (10, 40 and 70 K) and field (0-5 T) dependences of the flux pinning have been measured. The maximum field of irreversibility at 70 K is shown to change markedly upon both neutron and proton irradiations in some crystals and not others. The defect structure, chemistry and location in the unit cell has been determined in some cases. Some interaction with existing defect structure has been observed in proton and electron irradiations. The damage character and directionality has been determined in GeV ion irradiated crystals.

INTRODUCTION

The aim of this work is to understand the role of irradiation defects in producing changes in the properties of high temperature superconducting

materials. These changes can have practical advantages including small increases in T_c and quite large increases in J_c. One emphasis of this program is on determining the local atomic structure, chemistry and electronic state of these irradiation defects, while another parallel emphasis is on determining the interaction of these defects with magnetic flux vortices induced under applied magnetic fields. By combining TEM investigations with T_c and J_c measurements, and correlating results from the different recoil spectra produced by neutron, proton, and electron irradiations, we have investigated the pinning character of five different identified defect structures due to these irradiations. It is hoped that this will lead to the optimum irradiation/material conditions which produce the highest possible values of J_c while retaining the highest possible T_c. Perhaps more importantly, we will produce several different highly characterized and well understood defect states with which to probe and increase our understanding of the complex behavior of magnetic flux vortices in the high T_c superconductors.

To aid in the comparison of three of the four different irradiations discussed here, Figure 1 has been constructed. Illustrated are the recoil spectra in copper for 1 MeV electron irradiation, 3.5 MeV proton irradiation, and irradiation in the degraded fast neutron energy spectrum found in the graphite position H1 outside the core of the Missouri University Research Reactor (MURR). Recoil energies >10 keV are seen to constitute about 20% of the recoils for this neutron irradiation, and it is these high energy recoils which produce rather large (4nm) structurally disordered regions, or defect cascades, randomly in space, and which are visible in TEM and believed to be significant pinning sites for magnetic vortices. At the opposite extreme in distribution of recoil energies is that of 1 MeV electrons with a maximum recoil energy of only 70 eV in copper, sufficient to produce only single displaced atoms randomly in space. Proton irradiation produces a mix of recoil energies, but which are dominated by recoils of rather low energy <1000 eV, again distributed randomly in space. Not shown in this figure, but discussed in a later section, is the character of recoils and damage produced by heavy ions of very high energy (GeV), which will be seen to produce linear tracks of nearly continuous structural disorder along the entire ion path through the crystal ($\geq 20\mu m$).

The goal of this paper is to briefly review the results from a number of researchers associated with Argonne National Laboratory who are active in this field of flux pinning by irradiation defects, and to especially highlite several very interesting recent results. A more thorough review of the microstructural aspects of irradiations defects in YBCO can be found in ref. 3, and a thorough review of the flux pinning aspects of neutron irradiated high T_c superconductors can be found in ref. 4.

NEUTRON IRRADIATION

One of our primary tasks has been to investigate the defect structures produced by fast neutron irradiations using transmission electron microscopy (TEM) techniques. Much of this work is complete and is presented and discussed in detail in the Ph D thesis of Frischherz[5], with several papers on limited aspects[3,6,7] already published, and several more complete papers to be published shortly. Correlated with this TEM effort has been studies of flux pinning on neutron irradiated single crystals of YBCO by magnetization techniques[8].

To study systematically the effects of neutron irradiation on flux pinning, it is important to measure the increase in J_c as a function of neutron fluence. In this regard we have used the data of Sauerzopf et al[9] to select the range of fluence over which J_c changes substantially and then shows an approach toward saturation. This data, and especially the even more recent data presented in this conference by Sauerzopf et al[10], is extremely useful since it is on one single crystal which is irradiated and measured in dose increments, thus eliminating uncertainties due to crystal to crystal variations and changes in grain boundary properties. Based on the Sauerzopf data we selected neutron fluences of 2,4 and $8x10^{17}$ cm^{-2} (E_n>0.1 MeV) for TEM measurements, and $2x10^{17}$ cm^{-2}, a dose by which a substantial increase in J_c has occurred and before significant saturation behavior is noted, for further investigations of flux pinning by magnetization measurements.

An example of one result from the TEM work on neutron irradiated YBCO is shown in Figure 2. This composite of TEM micrographs qualitatively shows the build up of cascade defect density with dose, which was found to be linear with dose through this range within the accuracy of the measurement (±50%). The significance of this results is that while the cascade, or TEM visible defect density increases approximately linearly through this fluence range, the critical current density is beginning to show saturation behavior. The observed concentration of visible cascade defects at a neutron dose of $8x10^{17}$ cm^{-2} produces a defect spacing of about 30 nm in three dimensions, and this would seem to be sufficiently large to exclude saturation effects for pinning. This could imply that other defects, invisible in TEM, are also pinning, and their density is sufficiently high to produce an overlapping of pinning volumes. Or perhaps another mechanism becomes operable which decreases the effective strength of pinning due to degradation of other superconducting properties through this neutron fluence range. Evidence for the former, pinning by TEM invisible defects, will be presented, but whether their concentration

is sufficiently high to produce this saturation behavior in J_c is not known. A calculation of point defect density is in progress, and results may suggest a possible defect density of high magnitude. A completed calculation of cascade defect density yields a concentration of recoil events of energies >30 keV of about $2x10^{16}$ cm^{-3} at a neutron dose of $2x10^{17}$ cm^{-2}, surprisingly close to the TEM experimentally measured value of $1x10^{16}$ cm^{-3}.

A detailed study of the character of the cascade defects has been performed on both neutron irradiated YBCO and in ion simulation experiments[5]. Space limitation permits only a brief summary of these results. The sizes of the defect cascades produced by neutron irradiation range from 1 to 6 nm, with a mean size of about 3 nm. Strain fields extend out to about twice the defect size and are inwardly directed. A substantial fraction of defects show quite strong strain in [200] and weaker strain in [020]. In ion simulation experiments, the dominant structure of cascade defects is seen to be amorphous-like, with evidence in some for both coherent and incoherent recrystallization at the defect site. Detailed presentation and discussion of all these results will be published soon by Frischherz.

Recent annealing experiments have produced quite interesting results concerning the nature and stability of pinning defects produced by neutron irradiation. An example of recent work by Vlcek[8] is shown in Figure 3. Following neutron irradiation to $2x10^{17}$ cm^{-2} an annealing and measuring schedule was followed on three crystals, only one of which is illustrated. The central results are that a substantial fraction (90%, and in some crystals 100%) of flux pinning defects for H II ab are annealed through 300°C, but only about 50% are annealed for H II c. Correlated results from in situ and ex situ TEM annealing experiments, performed by Frischherz and preliminarily published[8], showed the visible cascade defects to be stable through this annealing. The present interpretation of these results are that pinning for H II ab is dominated by oxygen disorder on the basal or chain plane, probably in the form of oxygen deficient regions produced by recrystallized cascade defects rather than singly disordered oxygen atoms (at least by the time we can measure following neutron irradiation), and up to 50% of pinning for H II c must be due to TEM invisible defects such as isolated or small clusters of point defects, probably on or near the CuO_2 planes. The annealing of pinning defects for H II ab is almost certainly due to oxygen diffusion on the basal plane. One unanswered question is why the remaining defect cascades do not pin for this field orientation. The annealing of 50 % of pinning defects for H II c is the first result to suggest the importance of pinning by point defects or their clusters in neutron irradiated YBCO, but will be seen below to be confirmed by proton and electron irradiation results.

PROTON IRRADIATION

The design of the proton irradiation experiments has been much the same as that of the neutron irradiation experiments. Both TEM and magnetization techniques are again used to investigate defect structure and flux pinning enhancements produced by proton irradiation. The data of Civale et al[11], which measured changes in J_c as a function of proton fluence for single crystals of YBCO, has been used to select an optimum proton fluence at which to perform additional magnetization experiments and TEM investigations. This optimum fluence which produces near maximum increases in J_c is measuring temperature dependent, but near $1x10^{16}$ cm^{-2} at high temperatures (70-77 K). Our studies have centered on proton fluences of $1\text{-}2x10^{16}$ cm^{-2} with proton energy of 3.5 MeV (Civale used 3.0 MeV). Annealing experiments and comparisons with the results of neutron irradiations are also emphasized. These comparisons are strengthened by performing measurements on the same SQUID magnetometer with the same techniques, and using many single crystals from three sources, thus overcoming difficulties associated with crystal to crystal variations.

Examples of recent TEM micrographs are displayed in Figures 4 and 5. Figure 4 demonstrates that the defects formed by this 3.5 MeV proton irradiation to a fluence of $2x10^{16}$ are sensitive to small variations in imaging condition (s=0, s^+) and diffraction vector (G=200, 020). From these and other conventional TEM dark field micrographs has been learned that the most common visible defect has a highly anisotropic strain field (virtually none in G=020), and visible defect sizes and concentrations at this fluence are quite similar to those due to neutron irradiation at a fluence of $2x10^{17}$ neutrons/cm^2. Thus the main difference between defects produced by the two different types of irradiation appears to be in their structure and resultant strain field. In Figure 5 is a high resolution TEM micrograph where columns of the heavy cations, Y and Ba, are resolved in a nearly square lattice, and a single small defective area can be seen in the center. The structure in this defect can be seen to consist of bent or distorted lines of atom columns in the vertical direction, but not in the horizontal, both of which can be seen more easily when viewed at a very low angle along lines of atom columns (along the arrows). Thus the local atomic disorder of the heavy cations appears to be restricted to within (020) planes, but not between them. These (020) planes are, of course, perpendicular to the [020] directions which contain the Cu-O chains. This distortion and resultant strain is entirely consistent with the conventional dark field micrographs. Further high resolution TEM work is in progress to resolve the Cu sublattices, and also in the [100] and [010} orientations, which should provide additional detail on the atomic structure of these proton irradiation defects.

An important point regarding TEM results from in situ proton irradiation experiments should be mentioned. Observation of the annihilation of preirradiation defect microstructure (dislocations or stacking faults) under proton irradiation was made. This suggests an interaction between TEM invisible defects, produced and migrating under irradiation, with existing defect structure. However, no interaction with twin boundaries has been observed. The observed interaction is important to all our irradiation results, as will be shown below.

An example of results from a recent magnetization study of proton irradiated YBCO crystals[12] is shown in Figure 6. This annealing study shows recovery similar to neutron irradiated YBCO, but with a greater fraction recovered through 300°C. Also note at 70 K a huge change in the field value of reversible magnetization from the unirradiated to the irradiated crystal, in direct contradiction to results of Civale[11]. This has been found to be a crystal dependent result for both proton and neutron irradiations, and will be discussed below.

COMPARISON OF PROTON AND NEUTRON IRRADIATION

This comparison is mainly constructed for the two dose levels of $1x10^{16}$ protons (E=3.5 MeV) cm^{-2} and $2x10^{17}$ neutrons (E>0.1 MeV) cm^{-2}, both of which approach near maximum enhancements of J_c without significant saturation behavior at low measuring temperatures (5-10 K). Already mentioned is the similarity of defect sizes and concentrations visible in TEM. Some dissimilarity appears to exist in the visible defect structures themselves. This may result from the differences in recoil spectra shown in Figure 1, where the large fraction of intermediate recoil energies in the proton recoil spectrum may contribute a higher fraction of defects with highly anisotropic strain fields.

The higher fraction of quite low recoil energies in the proton irradiation is probably reflected in the annealing data, some of which is summarized in Table I. This table shows the annealed percentage of the irradiation induced increase in J_c, an average of three crystals in the proton[12] and neutron irradiations[8], and also includes a result from an electron irradiated crystal[13], which will be discussed more completely below. The main point of this table is the higher fraction of annealing for the irradiation with the higher fraction of lower energy recoils. The interpretation we place on this is that the annealing through 300°C of pinning defects is dominated by the recovery or annihilation of point defects or their small clusters (both mainly TEM invisible). The TEM visible cascade defects are stable through this temperature of anneal as mentioned above. Thus, the irradiated but unannealed J_c is enhanced by

point defect (or small clusters of point defects) pinning, even substantially in neutron irradiated YBCO. Note that the electron irradiated crystal displays a J_c approximately one half that of the other irradiations.

One of the most important results of the recent neutron and proton irradiation experiments is found in the comparison of both in Figure 7. The field variation in J_c at 70 K of 8 crystals, 5 neutron irradiated and 3 proton irradiated, are illustrated before and after irradiation to the previously defined doses. What is almost immediately obvious is how the preirradiation pinning structure has influenced a substantial portion of the irradiation enhancement of J_c for both types of irradiation. The three crystals which display reversible magnetization at 70 K above $5x10^3$ G before irradiation then display the largest irradiation enhanced J_c values and a large increase in the reversible field value, in contrast to other researchers to date. Those crystals with the larger J_c before irradiation display the smaller irradiation enhanced J_c and a nearly unchanged value of reversible field at 70 K, in agreement with the results of Weber[14] and Civale[11]. The crystals essentially fall into two groups. The existence of a preirradiation pinning structure may be related to some defect microstructure (as yet unidentified by TEM), which interacts with the irradiation produced defects in a way to prohibit the formation of a substantial fraction of pinning defects. Since there will be no difference in the production of all recoil energies among the different crystals, the most likely interaction is the suppression of mobility of point defects, which might otherwise cluster to form effective pinning centers. These pinning defects are apparently more effective at higher fields (at 70 K) than the defects cascades, which must be present to the same concentration in both type of crystals. The elimination of preirradiation pinning defects by the irradiation cannot explain this difference in pinning at an order of magnitude higher J_c. The most likely identity for this critical point defect has been determined by electron irradiation experiments described below.

ELECTRON IRRADIATION

A series of experiments have been performed by Giapintzakis et al[15] to investigate the formation of flux pinning centers by electron irradiation of single crystal YBCO. Several crystals were irradiated in a series of dose steps with 1 MeV electrons at room temperature. The maximum enhancement of J_c occurred near a fluence of 10^{19} electrons cm^{-2}, but a reproducible smaller peak in the dose curve was found at a fluence near 10^{18} cm^{-2}. In separate experiments a threshold energy for producing most of the pinning centers was found to be between 400 and 600 keV electron energies. Electron irradiation experiments at 600 keV on EuBCO and GdBCO single crystals (a substitution of heavier atoms for Y) proved that

the main pinning defect was not based on the displacement of Y, Eu or Gd in the unit cell-centered site. Also, the maximum recoil energy on the heavy Ba atom at this electron energy of 600 keV (about 12 eV) is probably too low for displacement. This leaves only the Cu and O atoms on the CuO_2 planes as likely candidates for displacement and creation of pinning defects for H II c. Using threshold energies and cross sections for both atoms, consistent with the threshold and dose data, it is possible to calculate the approximate concentrations of displacements of Cu and O atoms. Comparing these concentrations, which differ by a factor of 40 times more Cu displacements, with the calculations of Kes[16], it is found that Cu displacements are more likely to explain the measured J_c values than O defects,. as assumed by Kes. The smaller peak in the dose curve at 10^{18} cm^{-2} (E= 1 MeV) is then most likely explained by the formation of weaker pinning defects by displacements of Y or Ba atoms. A variation among crystals is explained by different amounts of clustering of these point defects determined by differing levels of preirradiation defect structure, an explanation consistent with observations of varying response of different crystals under proton and neutron irradiations, as discussed above. Visible TEM defects have not been found in several in situ electron irradiation experiments above a resolution limit of 2nm. High resolution TEM is in progress.

A recent result[17] tending to confirm the above interpretation, especially of the proton and neutron results of Figure 7, is shown in Figure 8. This electron irradiation with 1 MeV electrons to a dose of 10^{19} cm^{-2} illustrates the suggestion that the production and clustering of point defects can produce effective pinning defects which can dramatically raise the field of reversibility, in this crystal from <1T to >6T at 70 K.

GEV ION IRRADIATION

Quite recent developments with this new form of irradiation have revealed the unique nature of the pinning defects produced, perhaps the most effective pinning defects in YBCO at high temperatures and high fields, especially when the magnetic field is aligned along the ion irradiation direction. Again a collaboration with Civale et al[18] has given us the opportunity to investigate the nature of these defects using TEM techniques. A summary of work reported by Wheeler et al[19] is based on the ability to electropolish a small irradiated single crystal in two areas to two depths, thus investigating the damage character as a function of depth into the crystal. An example of this work is shown in Figure 9, where linear tracks of damaged material are formed along each ion path. It can be seen qualitatively that the tracks become less well aligned with the irradiation direction deeper into the crystal. The distributions of directions of about 100 tracks at both depths were determined and

compared with one of the leading computer model codes for ion irradiation of materials (TRIM[1]), where some difference was noted. Of special interest is the damaging mechanism, which is based on the transfer of ion energy into the material electronic system, primarily by ionization. The efficiency of transfer of this locally deposited energy from electron ionization into the atomic structure, locally disordering this structure, must be quite high. It is the atomic disorder which is imaged in TEM. These nearly linear, somewhat discontinuous tracks of atomic disorder are very effective pinners of magnetic flux vortices, especially at higher temperatures and fields.

SUMMARY

By combining observations by TEM and measurements of magnetization in single crystals of YBCO irradiated with neutrons, protons and electrons, we have made progress in determining the structure and flux pinning properties of various irradiation defects. Contributions to pinning of magnetic flux vortices by defect cascades in neutron irradiated samples, and by point defect processes under all irradiation conditions have been investigated by irradiation and annealing experiments. The displacement of copper atoms from the CuO_2 planes has been determined to produce significant pinning defects under electron irradiations, and by inference also under proton and neutron irradiations. Unusual pinning anisotropies have been found in all irradiation conditions. The influence of existing preirradiation pinning defects on both J_c enhancements and shifts in the reversible field values upon irradiation is demonstrated in eight different single crystals. A brief discussion of recent TEM results on linear defect tracks produced by 580 MeV Sn ion irradiation is given.

ACKNOWLEDGEMENTS

It is a pleasure to thank and acknowledge the efforts of Marcus Frischherz (ANL and Atominstitute, Vienna), Beatrix Vlcek (ANL), Hema Viswanathan (ANL and Purdue University), John Giapintzakis (University of Illinois), Bob Wheeler (ANL), and James Gledhill (University of Oxford, U.K.), who obtained most of the data. I also wish to thank my collaborators Harald Weber (Atominstitute, Vienna), Leonardo Civale and Alan Marwick (IBM), Don Ginsberg (University of Illinois), Marie-Odile Ruault (University of Paris, Orsay), Mike Jenkins (University of Oxford, U.K.), and George Crabtree (ANL) for much support and good advice. This work was supported by the U. S. Department of Energy, Conservation and Renewable Energy, and Basic Energy Sciences-Materials Science, under Contract No. W-31-109-ENG-38, the National Science Foundation-Office of Science and Technology Center for Superconductivity, under Contract No. STC-

8809854, and the Science and Engineering Research Council (U. K.) under grant GR/G43065.

REFERENCES

1. Ziegler, J. F., Biersack, J. P., and Littlemark, U., *The Stopping Range of Ions in Solids*, Pergamon Press, New York (1985) 79.

2. Greenwood, L. R. and Smither, R. K., ANL/FPP/TM (1985).

3. Kirk, M. A. and Weber, H. W., Electron Microscopy Investigations of Irradiation Defect Structures in the High T_c Superconductor $YBa_2Cu_3O_{7-x}$, in *Studies of High Temperature Superconductors* (Ed A. V. Narlikar) Nova Science Publishers, New York, vol 10 in press.

4. Weber, H. W. and Crabtree, G. W., Neutron Irradiation Effects in High-T_c Single Crystals, in *Studies of High Temperature Superconductors* (Ed A. V. Narlikar) Nova Science Publishers, New York, vol 9 in press.

5. Frischherz, M. C., Transmission Electron Microscopy of Radiation Induced Defects in the High Temperature Superconductor $YBa_2Cu_3O_{7-x}$, Ph D Dissertation, Technischen Universität Wien, 1992.

6. Frischherz, M. C., Kirk, M. A., Liu, J. Z., Zhang, J. P. and Weber, H. W., The Defect Structure of Ion and Neutron Irradiated $YBa_2Cu_3O_{7-x}$ Single Crystals, ASTM Symposium on "Effects of Radiation on Materials", Nashville, 1990, in press.

7. Kirk, M. A., Irradiation Defect Structures in $YBa_2Cu_3O_{7-x}$ and Their Correlation with Superconducting Properties, *Mat. Res. Soc. Symp. Proc.* Vol. 209 (1991) 743.

8. Vlcek, B. M., Frischherz, M. C., Fleshler, S., Welp, U., Liu, J. Z., Downey, J., Vandervoort, K. G., Crabtree, G. W., Kirk, M. A., Giapintzakis, J., and Farmer, J., Flux Pinning in $YBa_2Cu_3O_{7-x}$ Single Crystals: Neutron Irradiation and Annealing, accepted for publication in *Physical Review B*, 1992.

9. Sauerzopf, F. M., Wiesinger, H. P., Kritscha, W., and Weber, H. W., Neutron Irradiation Effects on Critical Current Densities in Single Crystalline $YBa_2Cu_3O_{7-x}$, *Physical Review B* (1991) 43 3091.

10. Sauerzopf, F. M., Wiesinger, H. P., Kritscha, W., Weber, H. W., Frischherz, M. C., and Gerstenberg, H., Fast Neutron Irradiation and Flux Pinning in Single Crystalline High Temperature Superconductors, this conference.

11. Civale, L., Marwick, A., McElfresh, M. W., Worthington, T. K., Malozemoff, A. P., Holtzberg, F., Thompson, J. R., and Kirk, M. A., *Phys. Rev. Lett.* (1990) 65 1164.

12. Viswanathan, H. K., Kirk, M. A., Baldo, P., Vlcek, B., Downey, J., and Crabtree, G. W., Annealing Effects on Flux Pinning and Critical Current Densities In Proton Irradiated $YBa_2Cu_3O_{7-x}$ Single Crystals, to be published.

13. Giapintzakis, J., to be published.

14. Weber, H. W., to be published in the *Proc. Internat. Workshop on Critical Current Limitations*, Zaborow, Poland, Oct. 1991, World Scientific, Singapore.

15. Giapintzakis, J., Lee, W. C., Rice, J. P., Ginsberg, D. M., Robertson, I. M., Wheeler, R., and Kirk, M. A., The Production and Identification of Flux Pinning Defects by Electron Irradiation in $YBa_2Cu_3O_{7-x}$ Single Crystals, accepted for publication in *Physical Review B* 1992.

16. Kes, P. H., Vortex Pinning and Creep Experiments, *Physica C* (1991) 185-189 288.

17. Giapintzakis, J., Kirk, M. A., Lee, W. C., Rice, J. P., Ginsberg, D. M., Robertson, I. M., Wheeler, R., to be published in *Proc. Mat. Res. Soc.* Symp. S, April 1992.

18. Civale, L., Marwick, A. D., Worthington, T. K., Kirk, M. A., Thompson, J. R., Krusin-Elbaum, L., Sun, Y., Clem, J. R., and Holtzberg, F., Vortex Confinement By Columnar Defects in $YBa_2Cu_3O_{7-x}$ Crystals: Enhanced Pinning at High Fields and Temperatures, *Physical Review Letters* (1991) 67 648.

19. Wheeler, R., Kirk, M. A., Brown, R., Marwick, A. D., Civale, L., and Holtzberg, F., TEM Study of Flux Pinning Defects in $YBa_2Cu_3O_{7-x}$ Produced by 580 MeV Sn Ion Irradiation, to be published in *Proc. Mat. Res. Soc.* Symp. A/H, Dec. 1991.

FIGURE CAPTIONS

1. Comparison of primary recoil energy distributions in irradiated copper, calculated for 1 MeV electrons using the McKinley-Feshback approximation for the Mott scattering cross section, for 3.5 MeV protons using TRIM[1], and calculated for fast neutrons in the H1 position in the Missouri University Research Reactor (MURR) by SPECTER[2], all assuming an arbitrary 20 eV threshold for defect production.

2. Composite of dark field TEM micrographs for the three neutron doses shown. Small black or black-white features about 5nm sized are cascade defects produced by the neutron irradiations.

3. Magnetic hysteresis loops for a crystal neutron irradiated to $2x10^{17}$ cm^{-2} ($E_n > 0.1$ MeV) and annealed. The pinning is so strong after irradiation of this rather large crystal that full penetration of the magnetic field is not achieved by 5 T with H ll c at 10 K.

4. Composite of dark field micrographs in the same area of a crystal proton irradiated to $2x10^{16}$ cm^{-2} imaged under different diffracting conditions. Defect strain fields are visible only in G=200 (arrowed) and require careful sample tilting to see (s=0 and s^+, a difference of about 0.1°).

5. High resolution micrograph of possible defect from proton irradiation, using 100 kV electron illumination which resolves only the nearly square heavy cation (Y, Ba) columns of atoms. The region of intersection of arrowed directions corresponds to the defect which is most easily seen by low angle viewing along the vertical direction.

6. Critical current as a function of field (H ll c) derived from Bean model analysis of magnetic hysteresis data for a crystal proton irradiated to $1x10^{16}$ cm^{-2} and annealed.

7. Comparison of J_c versus field (H ll c) for three proton ($1x10^{16}$ cm^{-2}) and 5 neutron ($2x10^{17}$ cm^{-2}) irradiated crystals, in the unirradiated (Unirr., top) and irradiated (Irr., bottom) states at 70 K.

8. Magnetic hysteresis loops measured at 70 K for a crystal before and after electron (1 MeV) irradiation to $1x10^{19}$ cm^{-2} .

9. Composite bright field micrographs taken under kinematic and systematic diffraction conditions, each tilted about 15° from [001], from

two depths in single crystal irradiated near [001] with 580 MeV Sn ions to 1.5×10^{11} cm^{-2} .

Table 1. Summary of neutron, proton and electron irradiations to "optimum fluences" and annealing to 300°C. Critical Currents are from magnetic hysteresis data for H ll c and H=2T.

Irradiations	Measuring Temperatures, °K	J_c(irrad), amps cm^{-2}	J_c(anneal)
Neutron	10	5×10^6	-40%
	70	3×10^5	-50%
Proton	10	7×10^6	-70%
	70	4×10^5	-60%
Electron	10	3×10^6	-100%

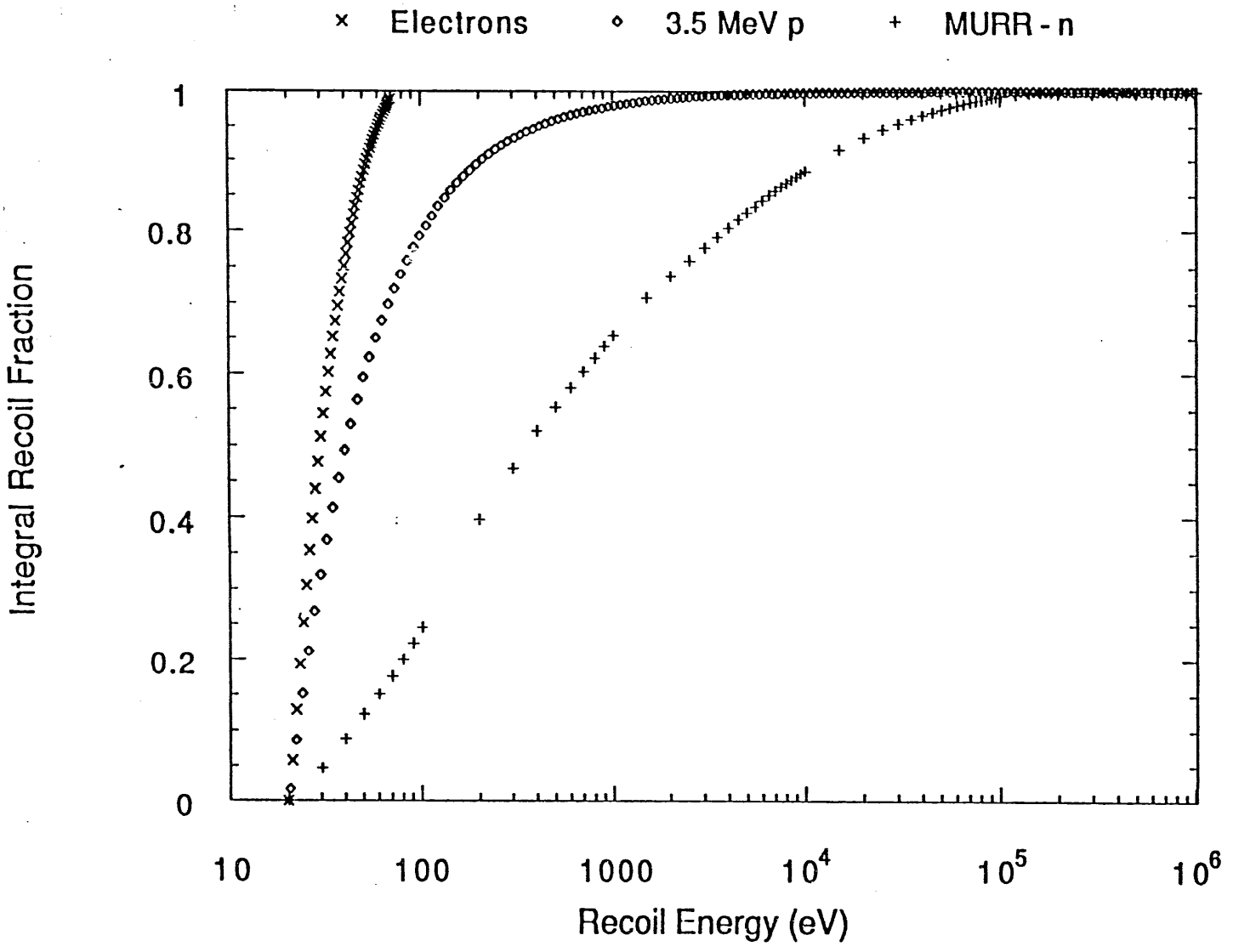
Electrons
3.5 MeV p
MURR - n
Integral Recoil Fraction
1
0.8
0.6
0.4
0.2
0
10
100
1000
10^4
10^5
10^6
Recoil Energy (eV)

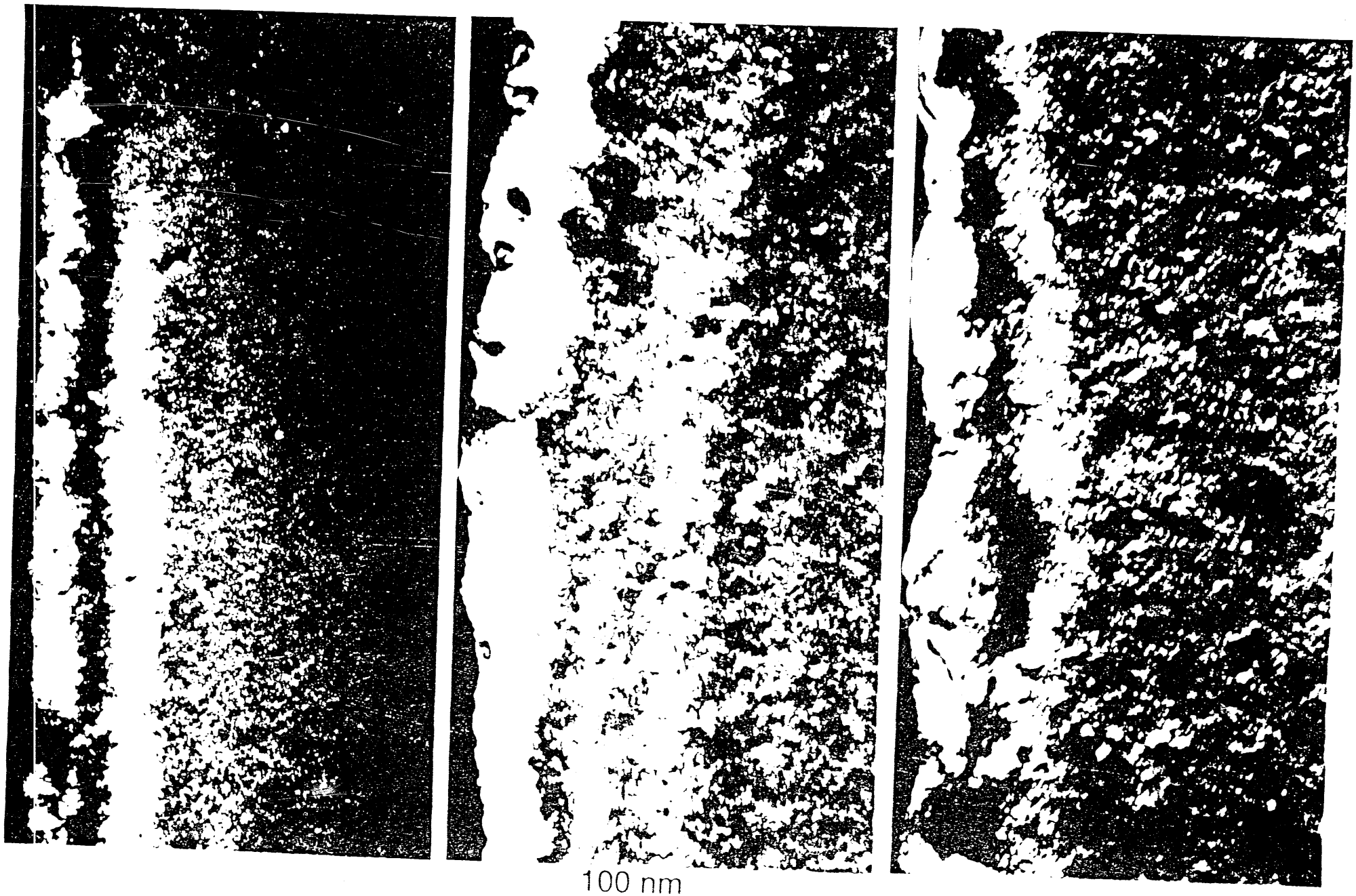

2×10^{17} n cm^{-2}
B = [010], g = 200

4×10^{17} n cm^{-2}
B = [010], g = 200

8×10^{17} n cm^{-2}
B = [001], g = 200

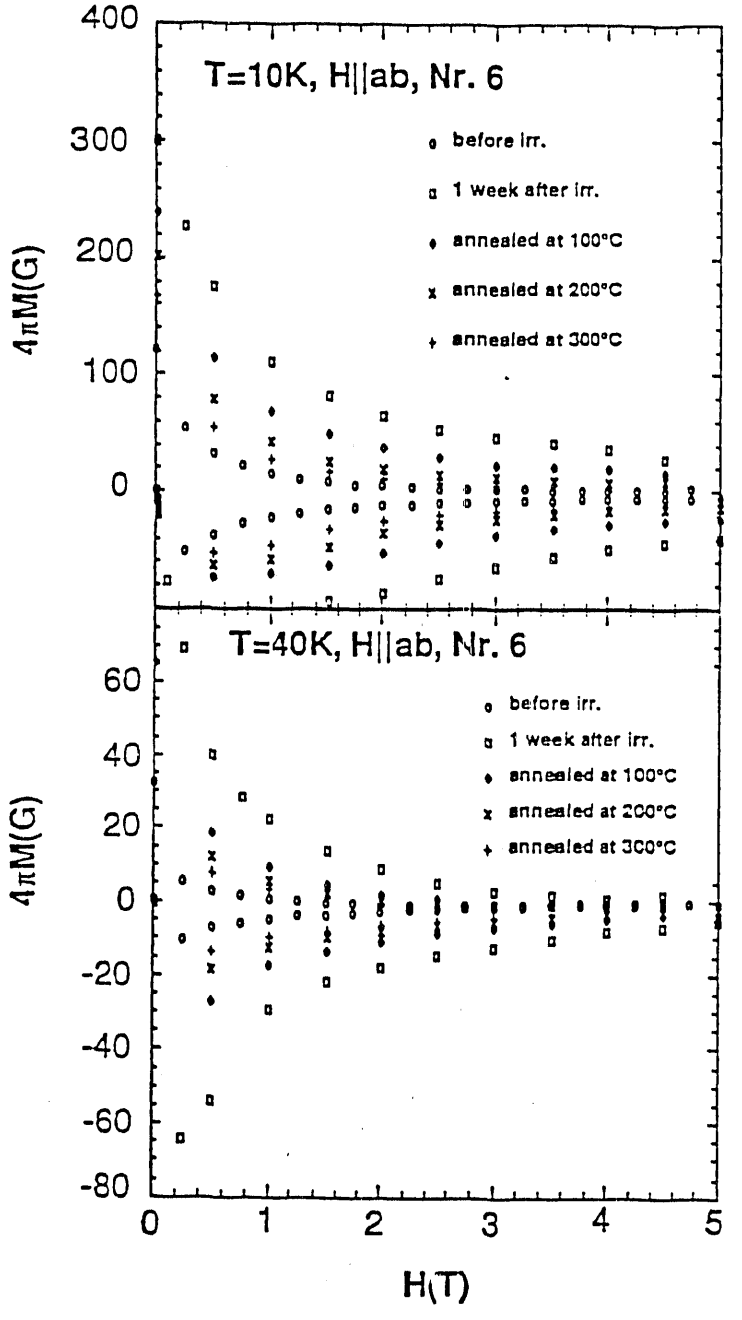
T=10K, H||ab, Nr. 6
before irr.
1 week after irr.
annealed at 100°C
annealed at 200°C
annealed at 300°C
4πM(G)
T=40K, H||ab, Nr. 6
before irr.
1 week after irr.
annealed at 100°C
annealed at 200°C
annealed at 300°C
4πM(G)
H(T)

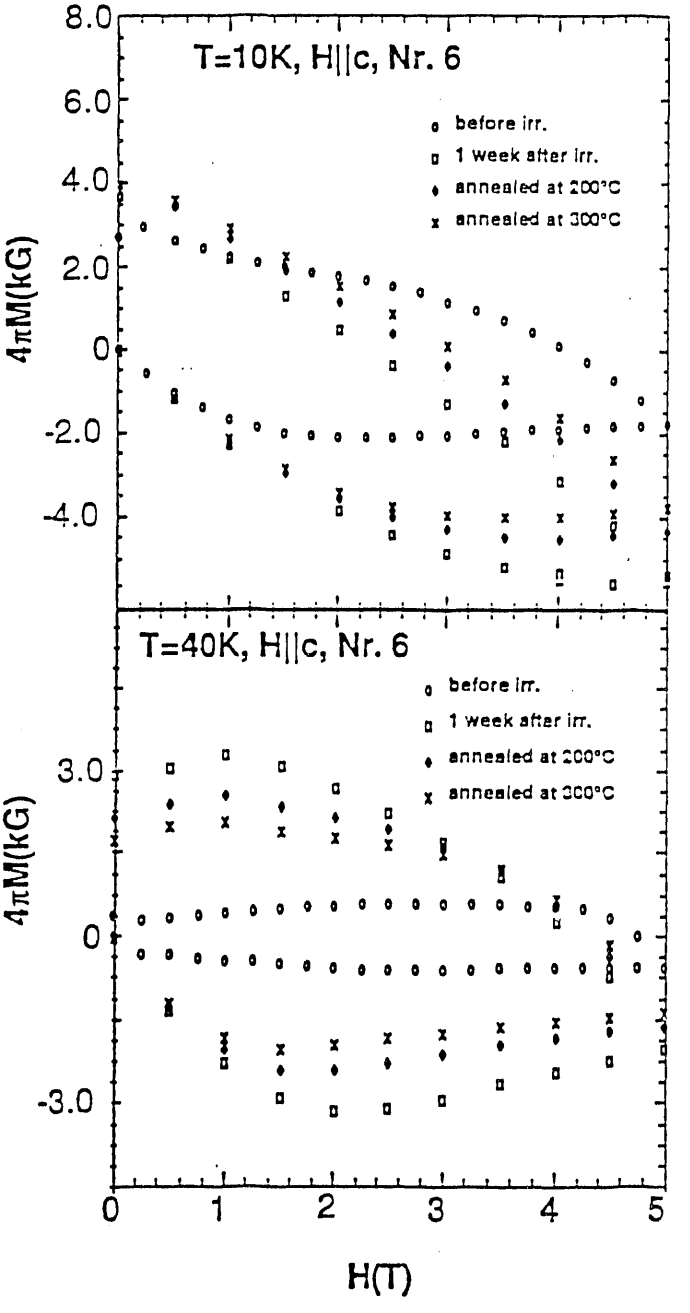
T=10K, H||c, Nr. 6
before irr.
1 week after irr.
annealed at 200°C
annealed at 300°C
4πM(kG)
T=40K, H||c, Nr. 6
before irr.
1 week after irr.
annealed at 200°C
annealed at 300°C
4πM(kG)
H(T)

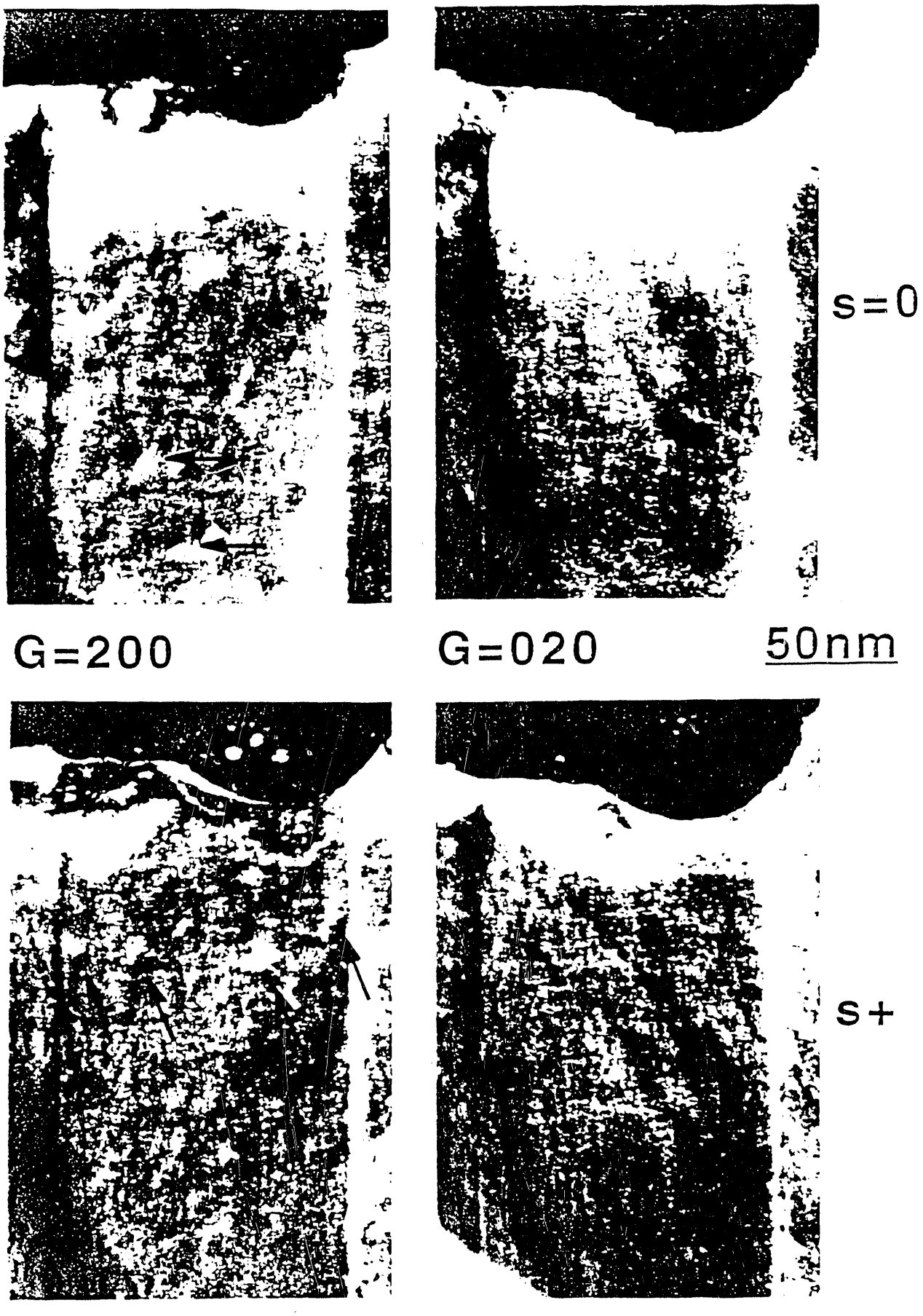
s=0
G=200
G=020
50nm
s+

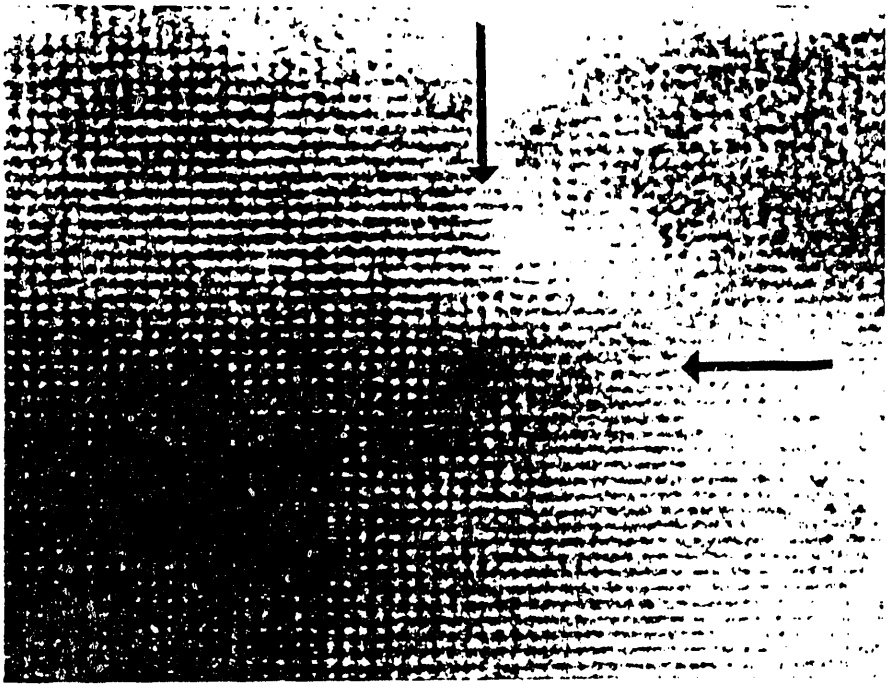

[001]

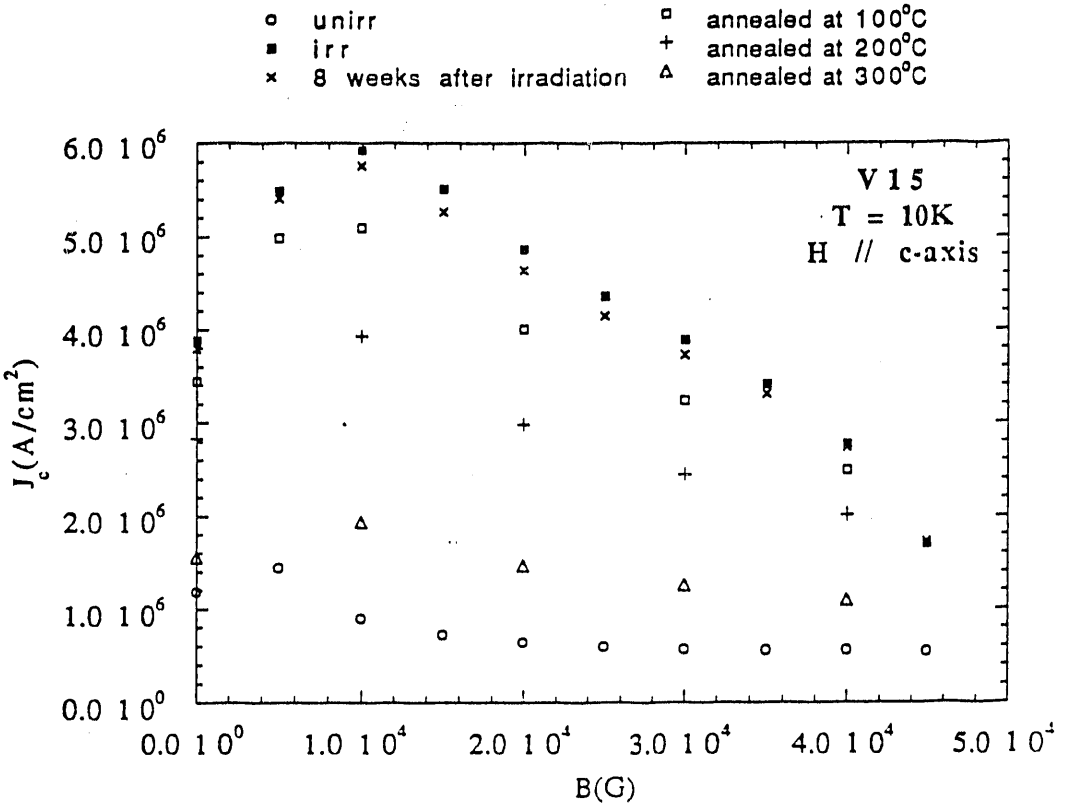
unirr
irr
8 weeks after irradiation
annealed at 100°C
annealed at 200°C
annealed at 300°C
V 1 5
T = 10K
H // c-axis
$J_c(A/cm^2)$
6.0 10^6
5.0 10^6
4.0 10^6
3.0 10^6
2.0 10^6
1.0 10^6
0.0 10^0
0.0 10^0
1.0 10^4
2.0 10^4
3.0 10^4
4.0 10^4
5.0 10^4
B(G)

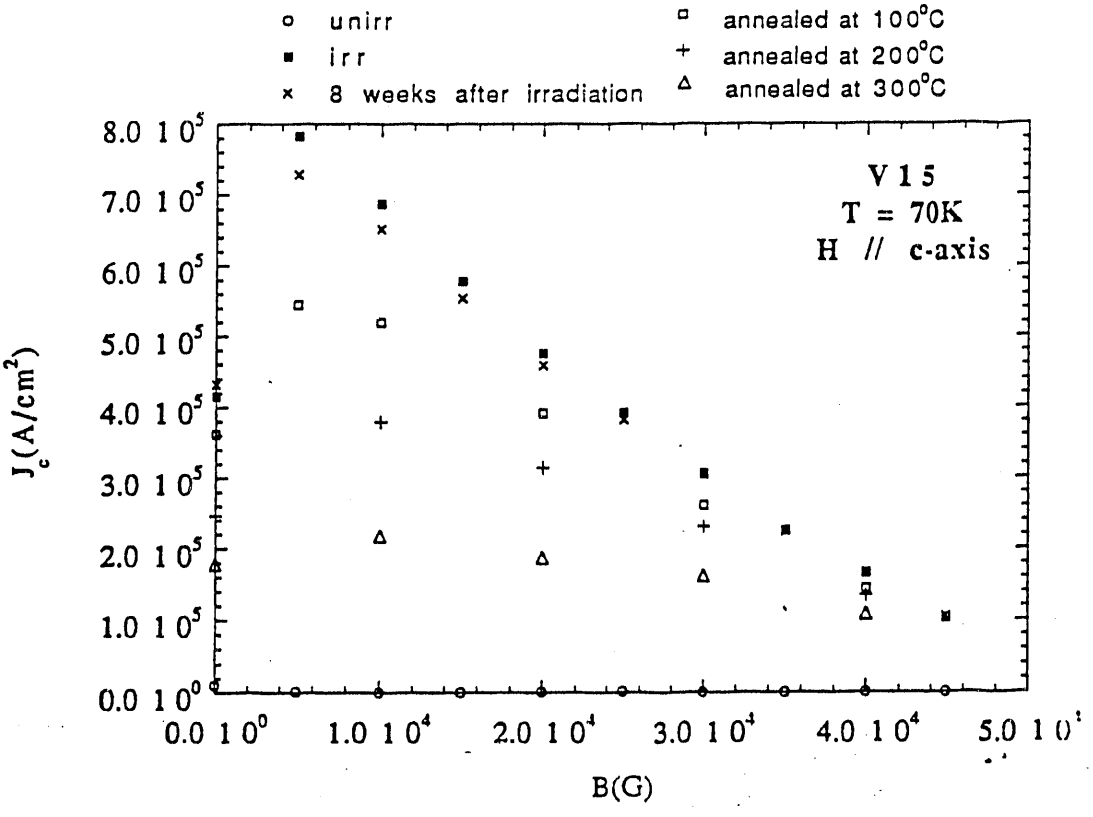
unirr
irr
8 weeks after irradiation
annealed at 100°C
annealed at 200°C
annealed at 300°C
V 1 5
T = 70K
H // c-axis
$J_c(A/cm^2)$
8.0 10^5
7.0 10^5
6.0 10^5
5.0 10^5
4.0 10^5
3.0 10^5
2.0 10^5
1.0 10^5
0.0 10^0
0.0 10^0
1.0 10^4
2.0 10^4
3.0 10^4
4.0 10^4
5.0 10^4
B(G)

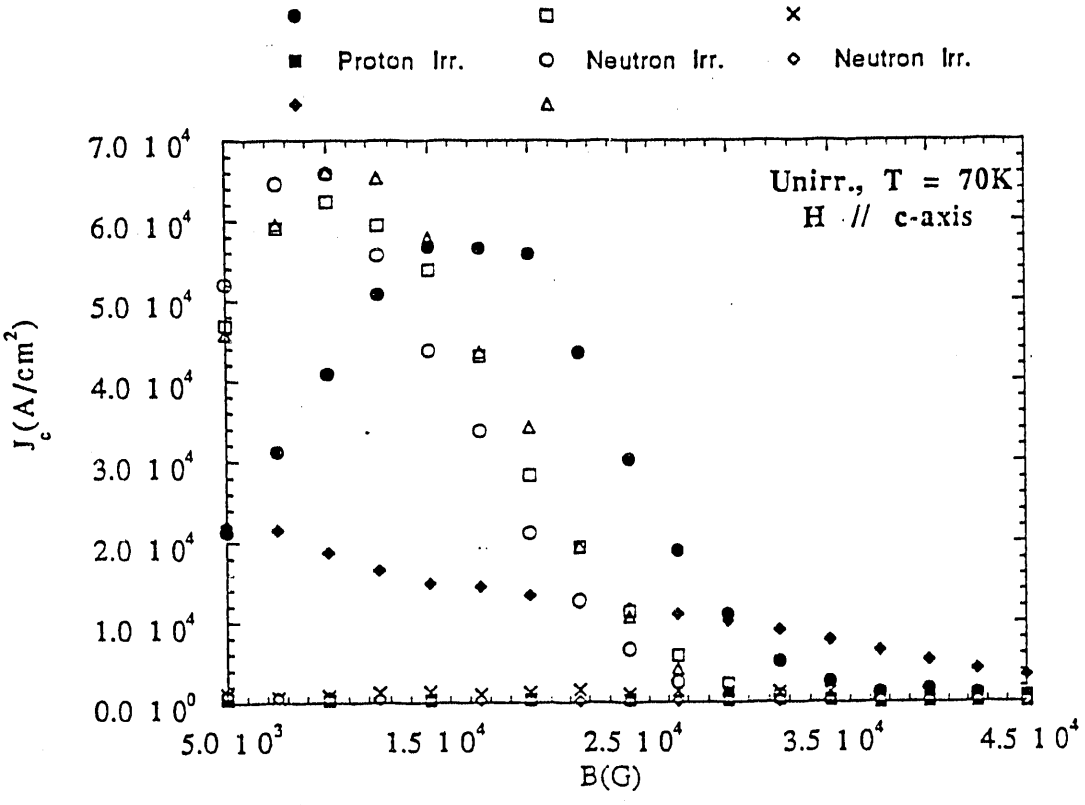
Proton Irr.
Neutron Irr.
Neutron Irr.
Unirr., T = 70K
H // c-axis
J_c(A/cm^2)
7.0 10^4
6.0 10^4
5.0 10^4
4.0 10^4
3.0 10^4
2.0 10^4
1.0 10^4
0.0 10^0
5.0 10^3
1.5 10^4
2.5 10^4
3.5 10^4
4.5 10^4
B(G)

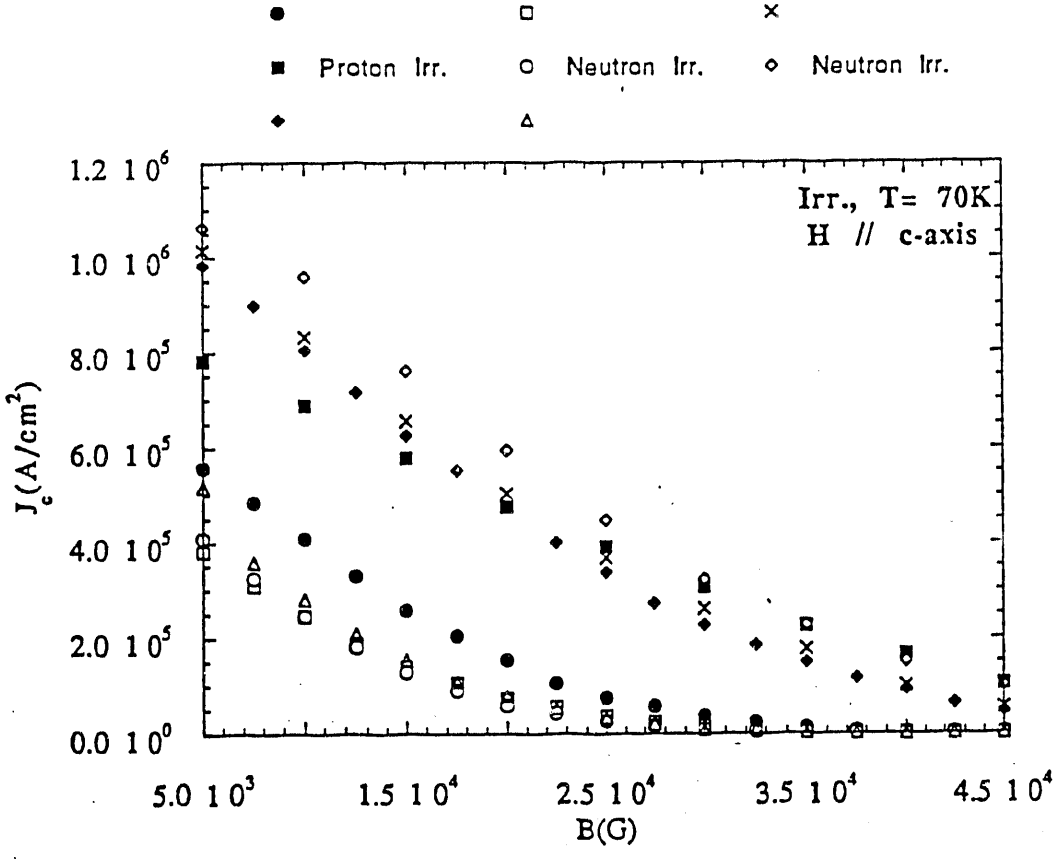
Proton Irr.
Neutron Irr.
Neutron Irr.
Irr., T= 70K
H // c-axis
J_c(A/cm^2)
1.2 10^6
1.0 10^6
8.0 10^5
6.0 10^5
4.0 10^5
2.0 10^5
0.0 10^0
5.0 10^3
1.5 10^4
2.5 10^4
3.5 10^4
4.5 10^4
B(G)

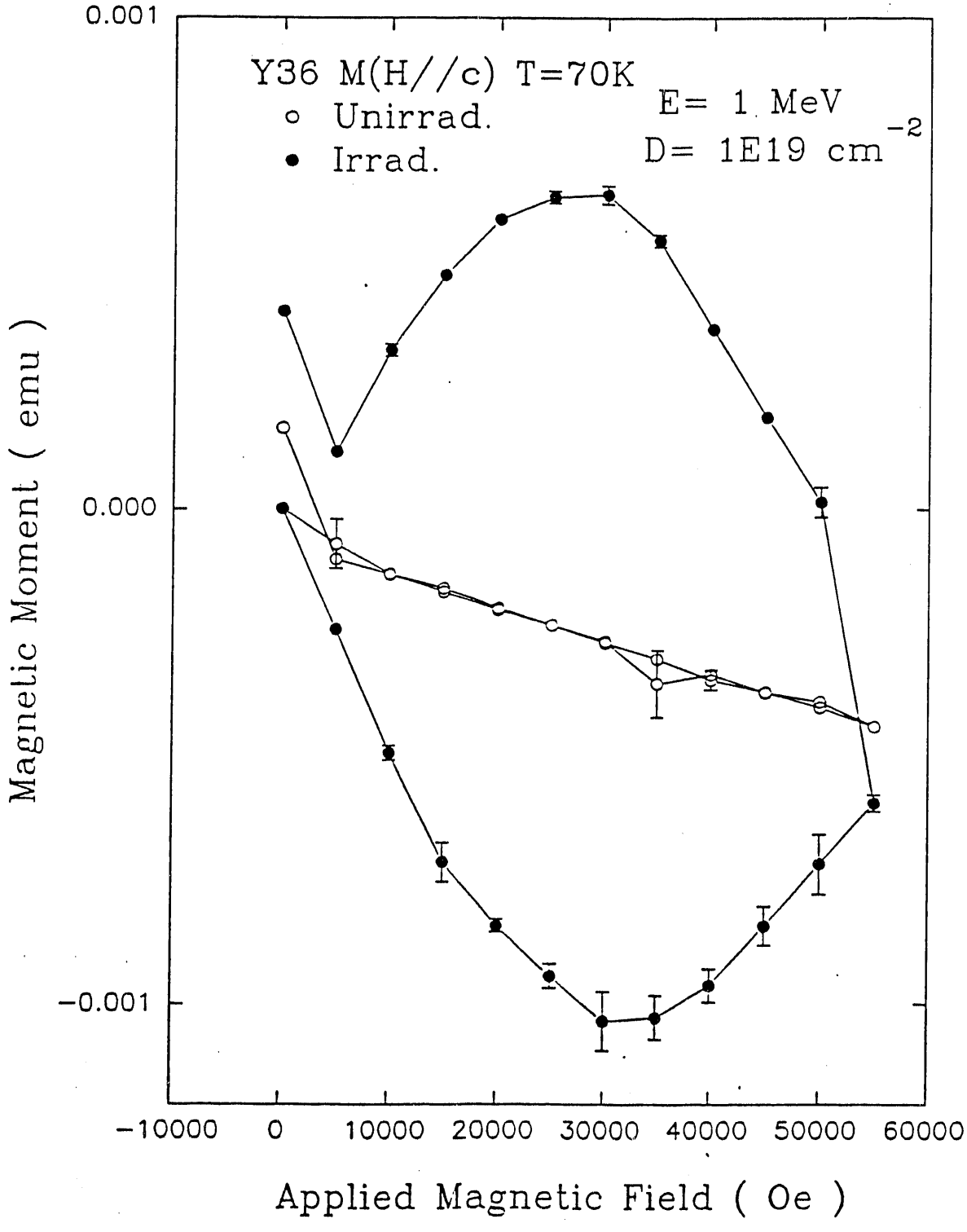
Y36 M(H//c) T=70K
Unirrad.
Irrad.
E= 1 MeV
D= 1E19 cm^{-2}
0.001
0.000
−0.001
Magnetic Moment (emu)
−10000
0
10000
20000
30000
40000
50000
60000
Applied Magnetic Field (Oe)

Fig. 9

DATE
FILMED
8/14/92